

ADAPTIVE BRIGHTNESS LEARNING FOR ACTIVE OBJECT RECOGNITION

Nuo Xu, Chunlei Huo, Chunhong Pan

1. NLPR, Institute of Automation, Chinese Academy of Sciences
2. University of Chinese Academy of Sciences

ABSTRACT

State-of-the-art object detection methods based on deep learning achieved promising performances in recent years. However, the performances are limited by the passive nature of the traditional object recognition framework in ignoring the relationship between imaging configuration and recognition performance as well as the importance of recognition performance feedback for improving image quality. To address the above limitations, an active object recognition method based on reinforcement learning is proposed in this paper by taking adaptive brightness adjustment as an example. Progressive brightness adjustment strategy is learned by maximizing recognition performance on reference high-quality training samples. With the help of active object recognition and brightness adjustment strategy, low-quality images can be converted into high-quality images, and overall performances are improved without retraining the detector.

Index Terms— object recognition, deep reinforcement learning, deep learning, remote sensing images

1. INTRODUCTION

Remote sensing image object recognition is to detect objects from remote sensing images and identify their types. It is challenging due to the difficulties in feature extraction, position regression and object classification. In recent years, deep learning provides great potentials for addressing the difficulties, and many promising approaches have been presented in literature. Generally, deep learning based approaches can be divided into the following two categories, two-stage methods(e.g., Faster RCNN [1, 2, 3] and R-FCN [4]) and one-stage methods(YOLO [5, 6, 7], SSD [8, 9] and RetinaNet [10]). The success of deep learning for remote sensing image object recognition is mainly contributed to the multi-layer nonlinear networks for learning representative features and the end-to-end mapping between images and their semantic labels.

Despite the effectiveness of deep learning, traditional object recognition approaches are limited due to the passive nature. Firstly, in the in-orbit imaging procedure, images are acquired with a focus on visual inspection performance, and the requirements specific to object recognition are not being taken into consideration. Secondly, images are directly used for

training or testing without proper image quality evaluation, or images are simply evaluated and reprocessed manually by visual inspection. In fact, requirements on imaging configuration for visual inspection and object recognition are different, and this gap will impact the object recognition performance. In other words, active object recognition is rarely considered in the in-orbit imaging procedure or the subsequent object recognition step.

To overcome the above limitations, an active object recognition approach is proposed based on reinforcement learning, and the role of reinforcement learning is to optimize imaging conditions for improving object recognition performance. It is worth noting that the application of reinforcement learning for image processing is a new topic and the proposed approach is different from related work[11, 12, 13]. Specifically, Caicedo[11] utilized reinforcement learning for direct object recognition, while the proposed approach utilizes reinforcement learning to generate better images for active object recognition within the traditional object recognition framework. Bellver[12] suggested applying reinforcement learning to focus attention on object candidates, but types of objects are not being considered and imaging configurations(such as brightness) are not changed. Most importantly, [11] and [12] use reinforcement learning alone to locate objects, but this paper combines deep reinforcement learning with the current mainstream deep learning object recognition algorithm. Park [13] suggested enhancing images by reinforcement learning for visual inspection instead of object recognition. In short, the proposed approach is different from related work, and the novelty of this paper is to enhance object recognition performance by actively improving image quality. Moreover, it is very useful for off-line recognition and on-line imaging.

2. THE PROPOSED APPROACH

Imaging configurations are important factors that affect image quality, among which the brightness is one of the most important factors that hinder later object recognition performances. Moreover, for different tasks such as visual inspection and object recognition, the metrics used for evaluating imaging configurations are different. For this reason, this paper studied active imaging configuration learning in the context of object recognition task by taking brightness learning as an example.

2.1. Problem Formulation

Environment, agent, state, action and reward are key components of reinforcement learning. Below, we describe each component in the context of active object recognition.

Environment. The environment of this paper refers to object detector D since the performance of action and reward is evaluated by it. For efficiency, YOLOv3 is used in this paper, but other object detectors such as SSD and Faster RCNN could be used without problem.

Agent. The role of the agent is to learn a series of environmental state-to-action mappings π according to the reward provided by the environment. For the agent, the basic learning rule is driven by the reward, i. e., if an action brings positive returns to the environment, this action will be strengthened, and vice versa.

State. The state S refers to the information that the agent uses to select the action. It is the feature F extracted from the image for agent training.

Action. The action A is defined as a global brightness adjustment operation, and it comes from the action space $\mathcal{A} = \{A_1, A_2, A_3\}$ (brighten, darken, termination), and the action that maximizes the overall expected reward when the algorithm converges is chosen by the agent at the next iteration.

Reward. Reward is provided by the environment to the agent for evaluating the quality of the actions. In this paper, the reward $R(t)$ is based on the recognition performances.

$$R(t) = \text{sign}(r(t) - r(t-1)) \quad (1)$$

Where $r = \frac{1}{2}(F + mIoU)$, $mIoU$ is the average IoU of all correct detection boxes, and F is the F-measure of the detection boxes with $IoU > 0.5$. By experiments, we find that the pure usage of F indicator and $mIoU$ does not work well. F indicator alone results in small reward, and $mIoU$ alone is less robust to multiple objects.

2.2. Automatic Brightness Adjustment

Based on the above denotations, our goal is to learn a best strategy (e.g., brightness adjustment action sequence $\{A_{opt}(t)\} \subseteq \{A(t) \mid A(t) \in \mathcal{A}, t = 0, 1, \dots, n\}$) to enhance the low-quality images and improve the recognition performance. In this paper, DQN[14] is used as the reinforcement learning framework to find the optimal strategy. Q function estimation is the most important step, and the state-action value function Q is

$$Q^\pi(S(t), A(t)) = E(R(t) + \gamma Q^\pi(S(t+1), A(t+1))). \quad (2)$$

Where γ is a discount factor, and the value of an action at step t is evaluated based on the reward of this step and the value of the next step. Considering that the state space is continuous and the approximation complexity is high, a six-layer fully-connected neural network is used as the Q-network. The

input of Q-network is the state feature F , which consists of two parts $F = (F_c, F_b)$, where F_c is the contextual feature extracted by the detector D and F_b the histogram of the image. In detail, F_c is the output of YOLOv3 on an image of the Darknet-53 layer, and its dimension is $13 \times 13 \times 1024$. By taking the average operation along the channel dimension, F_c is straightened into a vector of 169 dimensions. To compute the histogram, the RGB image is converted into the HSV color space, and a histogram is obtained on the component V , where the bin width is 4. Since the quantitative level is 256, a 64-dimension histogram can be obtained. Finally, the two parts are concatenated together to obtain a feature vector of 233 dimensions.

The flowchart of brightness adjustment process is shown in Fig. 1. The main strategy learning procedure is described as follows. At step t , an image $I(t)$ is represented by the contextual feature $F_c(I(t))$ and the brightness feature $F_b(I(t))$, and the image $I(t+1)$ is obtained by applying an action $A(t)$ on $I(t)$. Similarly, the input image $I(0)$ is enhanced by applying a series of adjustment actions $\{A(t) \mid A(t) \in \mathcal{A}, t = 0, 1, \dots, n\}$ iteratively, where $Q^\pi(S(t), A(t))$ is the output of Q-network with $S(t) = (F_c(I(t)), F_b(I(t)))$.

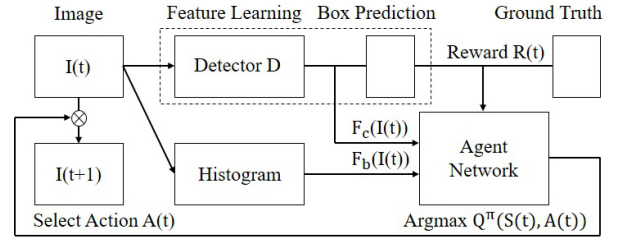


Fig. 1. Flowchart of the proposed approach.

Within the above reinforcement learning framework, one key problem to be solved is image brightness adjustment for later states transformation and action implementation. In this paper, images of different brightness levels are represented by a robust brightness transformation and a basic brightness image V_{base} . Below, we elaborate brightness transformation and action implementation in detail.

Brightness transformation For RGB image, its brightness degree is represented by a brightness level L computed on the image brightness component V in HSV color space. Brightness level lies within the range $[-1, 1]$, and changing brightness level means changing the image brightness. The negative number means that the image is dark, and the positive number means that the image is bright. The larger the absolute value, the darker or brighter the image.

To estimate brightness level for a component $V(t)$, a robust brightness transform is proposed (e.g., Eq. (3)).

$$V(t) = \begin{cases} (1 + L(t))V_{base} & -1 \leq L(t) < 0 \\ (1 - L(t))V_{base} + 255L(t) & 0 \leq L(t) \leq 1 \end{cases} \quad (3)$$

The method of multiplying a coefficient directly by $V(t-1)$ is not used for obtaining $V(t)$, the reason lies in the fact that pixels whose gray values are beyond 255 and being truncated in the brighten operation are difficult to be recovered in the later darken operation. The relationship between the pixel value of V_{base} and the pixel value of V under different brightness levels is shown in Fig. 2.

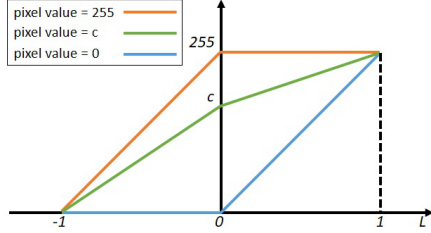


Fig. 2. Brightness transformation. This figure illustrates how the pixel value of V is adjusted under different brightness levels when the pixel value of V_{base} is 0, 255 and c , respectively.

For each image, V_{base} is the common basis, based on which the brightness component V of any level can be obtained by the above brightness transform. To compute V_{base} , without loss of generality, the histogram of V_{base} is assumed to be evenly distributed as shown in Fig. 3(a) and (b). 11 quantiles of the V component $\{p_0, p_{0.1}, p_{0.2}, \dots, p_1\}$ are used to roughly estimate the $L(0)$ of the original image by Eq. (4). The red dots in Fig. 3(a) and (b) are the quantiles of the histogram of original image.

$$L(0) = \frac{d}{255} - 1, \quad d \approx \frac{\sum_i p_i}{6} \quad (4)$$

As shown in Fig. 3(a) and (b), d refers to the length of the red line. The geometric interpretation of using quantiles to estimate d is also illustrated in the figure. After the quantiles are matched in pairs (such as $\{(p_0, p_1), (p_{0.1}, p_{0.9}) \dots\}$), the averaged sum of pairs is used as the estimated value of d , and the average operator is performed due to the fact that these sums are not necessarily equal. As for $V(0)$, it represents the V component of the original image. And according to Eq. (3), V_{base} can be calculated when $t = 0$.

Action implementation. The nature of action implementation is to change the image brightness level. From the brightness level $L(t)$, $L(t+1)$ is updated by Eq. (5). The cases that L lies out of the range of $[-1, 1]$ can thus be avoided. For bright images, the changing scope of L is greater in the darkening operation, and for dark images the changing scope of L is greater in the brightening operation, this is helpful for promoting the image in a good direction.

$$\begin{cases} L(t+1) = 0.95L(t) + 0.05 \times 1 & A(t) = A_1 \\ L(t+1) = 0.95L(t) + 0.05 \times (-1) & A(t) = A_2 \\ Termination & A(t) = A_3 \end{cases} \quad (5)$$

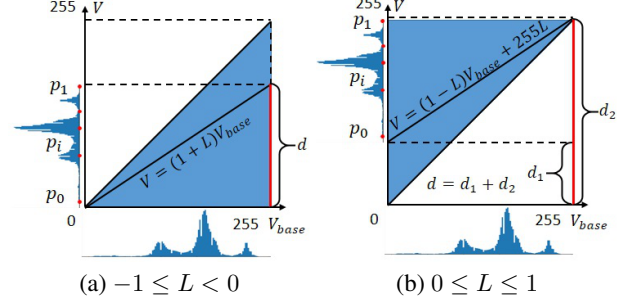


Fig. 3. V_{base} and brightness level estimation. (a): $-1 \leq L < 0$ (Linear mapping between the V component of a dark image and V_{base}). (b): $0 \leq L \leq 1$ (Linear mapping between the V component of a bright image and V_{base}).

3. EXPERIMENT

3.1. Experiment Setup

To illustrate the effectiveness of the proposed approach, experiments are conducted on a remote sensing image dataset Φ , which contains 25 aircraft categories. The dataset is consisted of 13,078 training images and 5,606 test images. The size of each image is 416×416 pixels. To demonstrate the effectiveness of active brightness learning, a different brightness transformation Eq. (6) is used to generate images of different brightness levels from the reference remote sensing images

$$V' = \begin{cases} \mu V & \text{darken } I \\ 255 - \mu(255 - V) & \text{brighten } I \end{cases} \quad (6)$$

According to Eq. (6), a new data set Φ' is obtained by sequentially setting μ to 0.6 and 0.3. Detector D is trained on Φ , but the agent is trained on $\Phi + \Phi'$.

The agent network is a six-layer fully connected neural network, and the neurons' number in each layer are 512, 512, 512, 512, 512, 3. Adam optimizer is employed for agent network learning with a basic learning rate of 0.001. The agent network eventually converges after 280,000 iterations, including 210,000 historical selection iterations and 70,000 back propagation iterations. Mini-batch size is set to be 32. Target network utilizes the soft update method with a factor of 0.001. YOLOv3 is chosen as detector D for strategy learning, and mAP is used to measure recognition performances. In the following sections, the performance on the reference dataset Φ is denoted as reference performance (RP), and the performance on the deteriorated dataset Φ' without brightness tuning is denoted as passive recognition performance (PRP), the performance on the deteriorated dataset Φ' with brightness adjusted by the proposed approach is denoted as active recognition performance (ARP).

3.2. Experiment Analysis

Table 1. Recognition performance comparison.

Model	Backbone	RP	PRP	ARP
YOLOv3[7]	DarkNet53	0.807	0.714	0.798
Faster RCNN[3]	VGG16	0.727	0.471	0.687
	ResNet50	0.730	0.507	0.677
R-FCN[4]	ResNet50	0.740	0.589	0.700
	ResNet101	0.749	0.577	0.711
SSD 300[8]	VGG16	0.802	0.539	0.580
RetinaNet[10]	VGG16	0.799	0.282	0.559
	ResNet50	0.795	0.401	0.643
	ResNet101	0.802	0.468	0.678

Performances of YOLOv3 on deteriorated images and adjusted versions are listed in the first row of Table 1. On the reference images, mAP is 0.807. However, mAP is reduced to 0.714 on the deteriorated images by the passive object recognition. This shows the importance and necessity of brightness adjustment. With the help of brightness adjustment, mAP on the adjusted versions is improved to 0.798, which is near the reference performance on the reference high-quality images. Some typical results are shown in Fig. 4, from which it can be seen that some objects failed to be recognized on the deteriorated image by passive object recognition strategy was recognized correctly by the proposed active object recognition strategy. Moreover, as illustrated in the images of the last two rows in Fig. 4, the performances on the adjusted images are even higher than that on the reference high-quality images, which illustrates the effectiveness and advantages of the proposed brightness adjustment approach.

Although the brightness adjustment strategy is learned driven by YOLOv3, however, it is promising for other detectors. For illustration, other four state-of-the-art recognition approaches and their variants were tested on Φ' , and brightness adjustment strategy driven by YOLOv3 is used directly for active object recognition. Performances of different detectors are listed in the other rows of Table 1. From Table 1, it can be observed that the performance improvement taken by YOLOv3 is better than other detectors, the reason lies in the fact that the brightness adjustment strategy is learned driven by YOLOv3 and YOLO is good at detecting small-size objects. For different detectors, PRPs on the deteriorated images reduced significantly. For instance, mAP of RetinaNet+VGG16 is reduced from 0.799 to 0.282. For the passive detectors, the degenerated performance is unacceptable for practical applications. In contrast, the proposed active object recognition strategy, ARPs are enhanced substantially. For example, mAP of Faster RCNN+VGG16 is improved from 0.471 to 0.687. These differences illustrate the universality of active object detection, and the universal-

ity is very important for online actively imaging procedure, i.e., if the brightness adjustment strategy is embed into the in-orbit camera, images acquired are promising for achieving higher recognition performance.

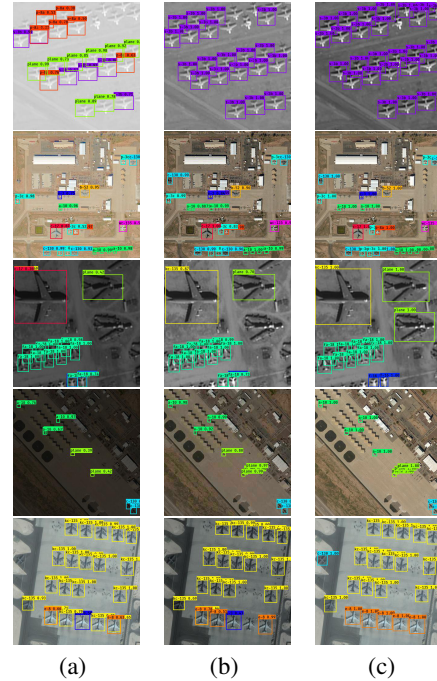


Fig. 4. Results comparison. (a): Passive object recognition, (b): Active object recognition. (c): Reference ground truth. The images in 1-2 rows are the adjustment cases on bright images, the images in 3-4 rows are the adjustment cases of dark images, and images in the 5th row are the adjustment cases on reference high-quality images.

4. CONCLUSION

An active object recognition approach is proposed in this paper, where a deep reinforcement learning strategy is used to help object recognition module actively adjust brightness. Experiments demonstrate the necessities of adaptive brightness adjustment and the effectiveness of the proposed active object recognition approach. The future work is mainly related to in-depth validation and further development in both the imaging procedure and object recognition procedure.

5. ACKNOWLEDGEMENTS

This work was supported by Beijing Natural Science Foundation (Grant No. L172053) and Natural Science Foundation of China (Grant No. 91646207).

6. REFERENCES

- [1] R. Girshick, J. Donahue, T. Darrell, and J. Malik, "Rich feature hierarchies for accurate object detection and semantic segmentation," in *Proceedings of the IEEE Conference on Computer Vision and Pattern Recognition (CVPR)*, 2014, pp. 580–587.
- [2] R. Girshick, "Fast r-cnn," in *Proceedings of the IEEE International Conference on Computer Vision (ICCV)*, 2015, pp. 1440–1448.
- [3] S. Ren, K. He, R. Girshick, and J. Sun, "Faster r-cnn: Towards real-time object detection with region proposal networks," in *Advances in Neural Information Processing Systems (NeurIPS)*, 2015, pp. 91–99.
- [4] J. Dai, Y. Li, K. He, and J. Sun, "R-fcn: Object detection via region-based fully convolutional networks," in *Advances in Neural Information Processing Systems (NeurIPS)*, 2016, pp. 379–387.
- [5] J. Redmon, S. Divvala, R. Girshick, and A. Farhadi, "You only look once: Unified, real-time object detection," in *Proceedings of the IEEE Conference on Computer Vision and Pattern Recognition (CVPR)*, 2016, pp. 779–788.
- [6] J. Redmon and A. Farhadi, "Yolo9000: Better, faster, stronger," in *Proceedings of the IEEE Conference on Computer Vision and Pattern Recognition (CVPR)*, 2017, pp. 6517–6525.
- [7] J. Redmon and A. Farhadi, "Yolov3: An incremental improvement.," in *arXiv preprint arXiv:1804.02767*, 2018.
- [8] W. Liu, D. Anguelov, D. Erhan, C. Szegedy, S. Reed, C.Y. Fu, and A. Berg, "Ssd: Single shot multibox detector," in *European Conference on Computer Vision (ECCV)*, 2016, pp. 21–37.
- [9] C. Fu, W. Liu, A. Ranga, A. Tyagi, and A. Berg, "Dssd : Deconvolutional single shot detector.," in *arXiv preprint arXiv:1701.06659*, 2017.
- [10] T. Lin, P. Goyal, R. Girshick, K. He, and P. Dollar, "Focal loss for dense object detection," in *International Conference on Computer Vision (ICCV)*, 2017, pp. 2999–3007.
- [11] J. Caicedo and S. Lazebnik, "Active object localization with deep reinforcement learning," in *Proceedings of the IEEE International Conference on Computer Vision (ICCV)*, 2015, pp. 2488–2496.
- [12] M. Bellver, X.G. Nieto, F.M. Acosta, and J. Torres, "Hierarchical object detection with deep reinforcement learning," *Advances in Neural Information Processing Systems (NeurIPS)*, pp. 137–163, 2016.
- [13] J. Park, J. Lee, D. Yoo, and I.S. Kweon, "Distort-and-recover: Color enhancement using deep reinforcement learning," in *Proceedings of the IEEE Conference on Computer Vision and Pattern Recognition (CVPR)*, 2018.
- [14] H. Van Hasselt, A. Guez, and D. Silver, "Deep reinforcement learning with double q-learning.," in *Association for the Advancement of Artificial Intelligence (AAAI)*. Phoenix, AZ, 2016, vol. 2, p. 5.